Superconducting Super Collider Laboratory
General Services
Technical Information and Publications
2550 Beckleymeade Avenue - MS 2002
Dallas, Texas 75237-3946
(214) 708-6044
FAX: (214) 708-6121

Date: November 13, 1992

To: Distribution

From: Technical Information and Publications

Subject: Addendum to SSCL-SR-1213

Please find attached, addendum to SSCL-SR-1213. The attached document is a complete paper titled "Calorimetry Subsystem R&D II" by James E. Brau. There are 21 pages in this addendum. This document is to be included as a complete paper and to become part of SSCL-SR-1213.

SSCL-SR-1213 Addendum

Calorimetry Subsystem R & D II*

James E. Brau

Addendum to the Proceedings of the 1991 Symposion on the
Superconducting Super Collider
The Project, The Progress, The Physics

Corpus Christ:
13-17 October 1991

15 November 1992

*Operated by the Universities Research Association, Inc., for the U.S. Department of Energy under Contract No. DE-AC35-89ER-40486.

Calorimetry Subsystem R&D II

James E. Brau
University of Oregon, Eugene, OR 97403

Abstract

This paper reviews the progress of SSC subsystem R&D on calorimetry with the technologies of:

- Barium Fluoride
- Scintillating Fiber
- Liquid Argon
- Liquid Xenon and Krypton
- Silicon.

The report generally covers progress on these projects through September, 1991.

Introduction

The physics requirements at the SSC challenge the performance of all detectors, including the calorimeters. The calorimeter issues can be factorized into electromagnetic issues and hadronic issues, many of which compete and require tradeoffs to be made between the optimizations. Here we review calorimetry R&D supported by the SSC subsystem R&D program. The projects included here were all of interest to the GEM Collaboration at the time of the review.[1] These are barium fluoride, scintillating fiber, liquid argon, liquid xenon/krypton, and silicon. This review presents an overview of the activities on each technology and relies on references for details.

Electromagnetic calorimetry

Electromagnetic calorimetry is crucial for many physics objectives of the SSC. One particularly important one is the search for the intermediate mass (~80 GeV to ~140 GeV) Higgs boson. Supersymmetric models favor a Higgs in this region. The dominant decay modes are swamped by backgrounds[2], and the unfavored decay to two photons becomes the most promising avenue for discovery, although the backgrounds are still challenging and potentially fatal.[3] Success demands excellent resolution and powerful background rejection, excellent resolution being about 1.0% energy resolution for a 100 GeV photon. This is an important goal for the GEM experiment.

Generally the energy resolution of a calorimeter can be expressed as

$$\sigma_E/E = (A/\sqrt{E} \oplus B)\%,$$

where A represents the stochastic term and B the constant term. Each calorimetry technique may achieve the 1.0% goal with a different balance in A and B. Table 1 shows the resolution

at 100 GeV for various values of A and B. This illustrates the solution to achieving one percent can come from differing emphasis on A and B. For example, at $E = 100\ GeV$

$$(2\%/\sqrt{E} \oplus 1\%) \approx (10\%/\sqrt{E} \oplus 0.25\%) \approx 1.0.$$

Note that in each of these examples the resolution is dominated by one of the two terms.

		B(%)			
		0.25	0.5	1.0	1.5
	2	0.32	0.51	1.02	1.51
	4	0.47	0.64	1.08	1.55
A(%)	6	0.65	0.78	1.17	1.62
	8	0.84	0.94	1.28	1.70
	10	1.03	1.12	1.41	1.80
	12	1.23	1.30	1.56	1.92

Table 1. The resolution function $\sigma_E/E = (A/\sqrt{E} \oplus B)\%$ at E = 100 GeV for values of A and B.

Hadronic calorimetry

Hadron calorimetry has advanced significantly in recent years.[4] All major high energy physics detectors are now designed with hadron calorimeters as essential components. The physics goals of such experiments include measurements and searches which require hadron calorimetry. The search for the Higgs boson at future colliders will rely heavily on calorimetry, hadronic as well as electromagnetic. For example, the most favorable limit on the mass of the Higgs boson at future hadron colliders may be obtained in the channel $WW \rightarrow l\nu jj$, provided WW-fusion events can be identified by tagging the two W-radiating quarks emerging with $p_T \sim M_W$.[5] The calorimeter will be required in this case to measure the jets from the Higgs decay and to tag the associated jets.

Searches for supersymmetric particles at future colliders will demand good measurements of missing energy, further driving calorimeter performance and design.[6] Compositeness studies will use the full performance of the calorimeters, with linearity of response being an important consideration in evaluating excess high transverse energy jets, which are the principal signature.[7]

The performance characteristics of hadron calorimeters include energy resolution, speed, linearity, hermeticity, spatial resolution, dynamic range, triggering capabilities, radiation hardness, reliability, and noise. Each of these must be evaluated in the context of physics goals. The physics requirements are fundamental and once set must lead the evaluation of calorimeter choices.

Summary of calorimetry requirements

Table 2 presents one version[8] of the general SSC physics requirements. Calorimetry at the SSC must provide energy measurements of electrons, photons, jets, and non-interacting particles such as neutrinos, and photinos by missing p_T. Calorimetry also must act as a particle filter, aid in particle identification, and measure muon energy loss. The requirements for calorimetry include survivability so that it can operate reliably and with little degradation of performance for periods of years at luminosities up to $10^{34} cm^{-2} s^{-1}$, dynamic range that stretches from muon measurements to decay products of very heavy Z's and high p_T forward jets, energy resolution that allows electromagnetic position measurements and high p_T jet spectra determinations for tests of compositeness, time resolution to correlate energy with beam crossings, segmentation which permits electron identification and reconstruction of $Z^0 \rightarrow jets$, total depth which reduces trigger rate for muons to an acceptable level, noise levels low enough to identify minimum ionizing particles and to identify isolated electrons, hermeticity sufficient to do missing E_T physics, and rapidity coverage wide enough to reduce missing p_T backgrounds.

Barium Fluoride

The BaF_2 Collaboration[9] (Caltech, UC-San Diego, Princeton, Carnegie Mellon, Brookhaven, ORNL, LANL, Shanghai Institute of Ceramics, Beijing Glass Research Institute, IHEP-Beijing, Tata Institute, University of Science and Technology - Hefei, China, and Tangji University, Sanghai) is developing barium fluoride as a very high precision electromagnetic calorimeter for the GEM experiment. Figure 1 illustrates the barium fluoride concept of GEM, containing 16,060 crystals (two pieces each) with $\Delta\eta = \Delta\phi \approx 0.04$. Each tower is 24.5 radiation lengths deep, coverage extends over $|\eta| \leq 2.5$ with a 10.3 m^2 calorimeter which weighs 50.2 tons. The inner radius is 75 cm and the inner length is 3 meters.

The BaF_2 Collaboration has assembled the first 7×7 pre-production prototype at Fermilab, where beam tests are being conducted. Facilities in China have been funded to provide a production capacity of 140 crystal pieces per month by the end of 1991. Full production will require 800 per month. A memorandum of understanding has been signed between the Shanghai Institute of Ceramics, the Beijing Glass Research Institute, and Caltech fixing the price for the final rad hard, mass mass produced crystals at $2.50 per cc.

An example of the uniformity of light collection which has been achieved for the crystals in the Fermilab beam test is shown in Figure 2. The special wrapping technique includes the use of black-painted aluminum mylar in the region near the phototube to suppress direct light. The wrapping is adjusted to get good uniformity. In Figure 2 the number of photoelectron per MeV for the 50 cm long BaF_2 crystal-pairs measured with a Cs^{137} source are shown. The deviation from flat corresponds to a variation over the region from 4 to 18 radiation lengths of 6.8%.

Parameter	Requirement	Basis of requirement
Survivability	Able to withstand 25 MR at $\eta = 3$ at R = 4m	Estimated 10 years of operation at the SSC
Dynamic Range	μ(minimum ionizing signal) 2-3 > pedestal? 4 TeV electromagnetic 6 TeV in jet cone	Linking central detector with μ system New Z' Test of compositeness
Resolution(linearity, stability, uniformity, calibration)	EM: $\frac{\Delta E}{E} = \frac{15\%}{\sqrt{E}} + 1\ \%$ ~1% at 100 GeV HAD: $\frac{\Delta E}{E} = \frac{50\%}{\sqrt{E}} + 2\ \%$	$\Gamma_{Z'}$ $h^0 \rightarrow \gamma\gamma$ Compositeness, Z→jj?
Time resolution	μ is minimum ionizing given the correct bucket	μ ID
	$E_{jet} > 20$GeV $\Delta t \leq 16$nsec	
Segmentation EM $\Delta\eta = \Delta\phi$ HAD Longitudinal Segmentation	 .02 .04 Not required	Z→jj perhaps position resolution Z→jj μ energy
Total Depth	8λ 11λ at η=0,14λ at η=5.5 ??	Compositeness μ ID SUSY
Position resolution	~ 1mm in EM	electron ID
Noise	MIP 2-3>Pedestal Electron isolation $E_T < 4$GeV in ΔR~0.2?	μ ID 4th Generation Family Top > 140 GeV
Hermiticity	$\not{E}_T \approx$ real ν background	H→ $\ell^+\ell^-\nu\bar{\nu}$ Light(250GeV) gluino
η range	$\lvert\eta\rvert < 5.5$	H→ $\ell^+\ell^-\nu\bar{\nu}$

Table 2. Physics Requirements for a Calorimeter at the SSC.

The Fermilab beam tests will study electron response for electrons from 10 GeV to $\geq$100 GeV in order to demonstrate the goal of

$$\sigma_E/E = (2.0/\sqrt{E} \oplus 0.5)\%.$$

Pion response will be measured, and electron-pion separation studied.

Radiation damage in the barium fluoride crystals is a serious problem which presents the critical research activity for the collaboration.[10] Studies of critical impurities are being conducted with a goal toward identifying and eliminating selected metals (such as cerium, lead, and cobalt) to less than one part per million, and eliminating O_2 and OH^- during pretreatment and growth. The radiation damage observed both from ionization and neutrons exhibits saturation after approximately 1-10 kRads, and can be annealed with either UV light or elevated temperature (for example, 500°C for 3 hours with no significant annealing occurring at room temperature.) Figure 3 shows results of neutron irradiation in the UC Irvine reactor and Co^{60} γ irradiation at JPL[9] on two 1" diameter × 1" long samples. The saturation and annealing effects are evident.

Confusing results abound in the data on damage effects in BaF_2. One example is illustrated in Figure 4 , which shows the scintillation emission spectrum for a 1 inch long BaF_2 crystal measured during irradiation at Brookhaven at 100 Rads and 10^6 Rads.[10] Here we see very little change in the emission spectrum. However, the transmission spectrum for this crystal did change, with a 30% decrease in light output observed. Such effects are under investigation.

The present evidence indicates that the radiation effects are most likely caused by impurities or defects.[10] It is <u>possible</u> that <u>pure</u> BaF_2 is intrinsicly very radiation hard. The present understanding of the radiation damage mechanism in BaF_2 identifies two aspects: 1.) there is an important role of cationic impurities (eg. lead, cerium), and 2.) oxygen absorption contributes. Therefore the path toward improvement includes the use of higher purity crystals and controlling the pretreatment in order to remove oxygen. A controlled furnace atmosphere could also be crucial.

GEM has established an expert panel with membership experienced in radiation effects in scintillating materials and knowledgable on the crystal production. This panel is assessing the prospects for finding a solution to this problem by summer, 1992, in time for GEM to make a decision for its calorimeter. If GEM proceeds, the panel will advise the GEM collaboration on its R&D plan leading up to that decision.

Scintillating Fiber

The SSCintCal Collaboration[11] (Boston, Drexel, Fairfield, LSU, Michigan State, Texas A&M, UC-San Diego, Draper, FNAL, and LLL) is pursuing scintillating fiber calorimetry in the US and collaborating with the CERN work with the SPACAL Collaboration. Part of this group has participated in the SPACAL CERN beam tests to 150 GeV where improved electromagnetic resolution consistent with EGS and with a decreased constant term of 0.4% has now been observed.[12] This result (see Figure 5) comes with smaller diameter fibers

(0.5 mm) and projective geometry. Further improvement in the electromagnetic resolution (to $4\%/\sqrt{E}$) is anticipated by this group with the increase of the sampling fraction from 20% (the fraction motivated by compensation) to 50%.

A new fabrication technique using low temperature casting has now been fully developed for projective hadronic calorimeter towers.[13] For one ton towers (representing $\Delta\eta \times \Delta\phi = 0.1 \times 0.1$) are being cast for the Fermilab beam test at the end of 1991. There modules are driven for use in the GEM calorimeter, where scintillating fiber is one of the options for the hadron calorimeter.

A study of radiation damage to scintillating fibers has shown a preferable fiber choice.[14] Figure 6 shows the light output of three different types of fibers before irradiation and after exposure to 9 MRads of Co^{60}. These studies were also conducted for neutrons up to 1.2×10^{13} n/cm^2. The neutron damage results in about 10 % light loss, which translates to a 0.5% constant term without annealing, and less with annealing.

The SSCintCal Collaboration has developed a fiber welding machine which operates at 10 sec/joint in order to build dichroic towers. They have produced such laminated towers which give chromatically separated electromagnetic and hadronic signals. These modules bring the first 28 cm of the calorimeter (electromagnetic) out on green fibers and the last 180 cm (hadronic) out on blue fibers. Tests are underway.

As a further contribution to the SPACAL effort, two 2 m laminated, projective towers where constructed in the US and tested with SPACAL last summer. Analysis is in progress.

Liquid Argon

The SSC Liquid Argon Collaboration[15] (Adelphi, Arizona, Brookhaven, Florida State, Iowa State, KEK, Tokyo Institute of Technology, LBL, Maryland, Martin Marietta Astronautics, Michigan State, Mississippi, ORNL, Rochester, SSCL, Tennessee, and Washington) builds on many years of development of liquid argon calorimeters. These many years of experience have created a mature technology, the first strength of this choice for an SSC calorimeter. There are several other often stated strengths of liquid argon as a calorimeter readout medium. These include the property of unit gain with linear response which guarantees good stability, easy calibration leading to good energy resolution, the inherent radiation hardness of the technique, and the easy of segmentation of the active medium. The most significant difficulty for this technique is the slow response time, with a drift velocity of about 5 mm/sec. This means it takes about 400 nanoseconds to drift through a typical gap of 2 mm. In 100 nanoseconds, however, one can still collect more than forty percent of the charge with some loss in signal to noise. The leading edge of the pulse, nevertheless, can be used to determine the timing to a beam crossing.[16]

One focus of the liquid argon group during the past year has been to build a liquid argon calorimeter with fast shaping to measure the resolution, e/π and pileup. Electronics based on the HELIOS design[17] with shaping times of 50 nsec, 100 nsec, ~125 nsec, and 200 nsec was built. The hadron calorimeter was built with 12 mm thick lead plates.[18] The calorimeter is 1 meter × 1 meter in cross section and 96 layers deep for a depth of about 7.5 interaction lengths. Each unit cell consists of the 12 mm lead plate, a 2 mm liquid argon

gap, a readout board, and a 2 mm liquid argon gap. Each readout board has 40 2.5 cm × 1 meter readout strips, with alternate layers having horizontal or vertical strips. There are 240 readout channels, as the strips are ganged to give three horizontal and three vertical readouts in depth. The comparison of many characteristics of this calorimeter with those of HELIOS[17] are shown in Table 3.

characteristic	HELIOS	LAC
absorber	3.4 mm ^{238}U	12 mm Pb
depth	4.5λ	7.5 λ
cross section	120 cm × 120 cm	100 cm × 100 cm
LA gap	2.5 mm	2.0 mm
readout	48 × 2.5 cm strip	40 × 2.5 cm strip
sampling ratio	12%	5%
number of cells	10	16
transformer ratio	11:1	12.5:1
feedback capacitor	5 pF	5 pF
shaping time	134 nsec	50, 100, 200 nsec
mv/GeV	1.8	1
charge transfer time	~ 35 nsec	~ 25 nsec

Table 3. Comparison of HELIOS and SSC subsystem (LAC) liquid argon calorimeters.

The calorimeter was tested at Brookhaven with electrons and negative pions from 500 MeV/c to 20 GeV/c. The preliminary results[18] for the electron resolution are:

$$\sigma_e/E_e = (0.212 \pm 0.0027)/\sqrt{E_e}$$

except at the lowest energies where the suppression of the electromagnetic shower in the 12 mm thick lead plates has a significant effect on the response. Below 1 GeV the electron response falls below a linear extrapolation from higher energy and the resolution degrades, being 30% at 1 GeV. The pion resolution is found to be:

$$\sigma_\pi/E_\pi = (0.612 \pm 0.015)/\sqrt{E_\pi}.$$

The energy dependence of e/π is shown in Figure 7.

The response is found to be linear for all shaping times, the e/π ratio is 1.17 at 20 GeV, and the resolution results agree with simulations from EGS and CALOR89. The noise was

measured to be ~ 100 MeV for each of the 240 channels for the digital output shaping time of ~ 125 nsec. Timing resolution for 20 GeV pions was found to be 4 nsec.

A study completed this year by Mockett et al. has shown the potential for good $\gamma - \pi^0$ discrimination in a liquid argon parallel plate electromagnetic calorimeter employing 1 mm readout strips in two orthogonal directions. Studies of this approach and others have shown that to be effective in separating single gammas and two from π^0s in searching for an intermediate mass Higgs boson, the 1 mm strip is necessary. For example, Figure 8[19] shows the spectrum of accepted gammas in a 100 GeV Higgs search in the GEM detector (calorimeter inner radius of 75 cm), with superimposed curves to show the probability that the two gammas from a π^0 of a given value of P/L (P is the π^0 momentum and L is the distance to the calorimeter from the interaction point) separate by 6 mm, 3 mm, or 2 mm in either of two orthogonal directions at the calorimeter. A detector able to separate two gammas separating by no less than 6 mm is seen to fail to cover the desired parameter space, while a preradiator succeeding for gammas opening by 2 mm does very well. This calls for a 1 mm strip system. Figure 9 shows the simulated results from a study of the liquid argon strip readout.[20] In this study, every sixth strip was connected to hold down the number of readout channels. As Figure 9 shows, this does not cause a problem for the performance.

The liquid argon subsystem group also produced the SDC Conceptual Design Report[21] this year. SDC has chosen not to use the liquid argon calorimeter, although they concluded it was a viable system at the SSC.

Liquid Xenon and Krypton

Work has progressed on scintillating liquid xenon and liquid krypton electromagnetic calorimeters[22] (MIT, Columbia, Washington, ITEP-Moscow, IHEP-Serpukov, Waseda University, Saitama College of Health, Riken, and Institute of Atomic Energy-Beijing). This work is motivated by the speed of these noble liquids, the large light output (4-7 $\times 10^7$ γ/GeV), the radiation hardness, the homogeneity, and the low critical energy, The major difficulty is the uniformity of light collection in the long cells.

There are three modes of application under investigation:

1. homogeneous with entire volume active;
2. sampling with active medium sandwiched between absorbers;
3. and scintillating homogeneous front section followed by sampling section.

For testing the homogeneous application, the collaboration is constructing a single cell and 7×7 cell calorimeters. They are also designing a pointing ionization sampling calorimeter based on the accordion concept developed at CERN for liquid argon[23] with an additional homogeneous pre-radiator in front. The scintillation light in the front end homogeneous section of a few radiation lengths would be read out, while the ionization in the back accordion section would provide the rest of the signal. This SandI concept could provide a pointing ionization sampling calorimeter with a very fine detailed preradiator to discriminate γs from π^0s.

Finally, this collaboration is beginning an investigation of the Liquid Xenon SPACAL (Macaroni) using small kapton capillaries coated with MgF_2 and filled with liquid xenon.

Total internal reflection in liquid xenon against MgF_2 walls has been seen experimentally.[24]

Fundamental to this concept is the use of UV diodes. Fast UV diodes and matching amplifiers have been tested in liquid with beams this year.

Silicon

The Silicon Electromagnetic Calorimeter Collaboration[25] (Brookhaven, Carnegie Mellon, Universitat Hamburg, IntraSpec, Moscow State, ORNL, Oregon, Tennessee) is developing silicon calorimetry and preradiators for the SSC. The collaboration is building an electromagnetic calorimeter and a silicon preradiator prototype instrumented with fast ASIC electronics and has undertaken a number of radiation damage studies.

The electromagnetic calorimeter is constructed with three different diode pad sizes. Silicon arrays of 64 mm × 64 mm area are subdivided into 4, 16, or 36 square diodes cells of 3.2 cm × 3.2 cm, 1.6 cm × 1.6 cm, and 1.1 cm × 1.1 cm area each. The different sizes span the interesting calorimetry cell sizes from the needs of a hadron calorimeter (as in L^*) to an EM calorimeter or preradiator (as in EMPACT/Texas or GEM). Each diode of the calorimeter has a preamplifier mounted directly above it. The preamplifiers are charge-sensitive bipolar preamplifiers developed by the ORNL group. Table 4 summarizes the characteristics of these preamplifiers as simulated after design. Different preamplifier designs are optimized for different detector sizes (1 × 1 refers to $1cm \times 1cm$, 2 × 2 to $2cm \times 2cm$, and so on).[26]

Preamp Type	Folded Cascade			Current Feedback		Differential	
Detector Size	1 × 1	2 × 2	3 × 3	1 × 1	2 × 2	3 × 3	4 × 4
$C_d(pF)$	27	108	243	27	108	243	432
ENC_e	4152	5001(6167)	7868	7619	9023(7971)	13,750	19,200
$P_d(mW)$	18.2	19.5(17.4)	19	15	15(15.3)	23.5	23.5
$t_R(nsec)$	3.5	3.3	5.4	2.4	6.7	5.6	4.2
Ext. Cap.?	NO	NO	NO	YES	YES	YES	YES

Table 4. Simulation results for the Charge-Sensitive Bipolar Preamplifiers using Harris' VHF Process

The group is also building a silicon preradiator prototype using the same detectors and electronics. Studies done in the past year have shown that what is needed for the preradiator is the ability to separate two electromagnetic showers within a few millimeters at the calorimeter (see discussion under liquid argon and Figure 8). Therefore, the group will apply the experience gained from the preradiator prototype based on the pad configuration to a preradiator based on milli-strip arrays of 64 mm × 1 mm.

Much of the effort of the silicon group has focussed on understanding radiation damage. The two approaches to this issue have been addressed: 1.) the effect of radiation on the silicon detectors, and 2.) controlling the materials to improve radiation hardness.

The investigations into the effect of radiation emphasize neutrons, with studies up to fluences of 10^{15} n/cm^2. These studies concentrate on the changes in effective impurity concentration with increased fluence, and room temperature annealing.[27] Figure 10 presents the C/V characteristics of planar/surface barrier type detectors fabricated at Hamburg from 6 kΩ n-type Wacker silicon of thickness 400 μm. These characteristics have been measured immediately after irradiation. The depletion voltage is seen to drop from 75 volts to 12 volts at 3×10^{12} n/cm^2, and then increase again. Figure 11 shows, interestingly, that at high fluences these curves follow a universal shape when normalized to the bias voltage. From these data, the net damage affected impurity concentration has been extracted, resulting in Figure 12. This curve is interpreted as resulting from the removal of the phosphorus donors and boron acceptors, and the generation of acceptor like defects, with the notable inversion from n-type to p-type. It must be mentioned that this observation of inversion was not confirmed by parallel studies within the group.[28]

The materials study program aims at understanding the controlled introduction or removal of impurity concentrations or structural defects to improve radiation hardness.[29] Figure 13 shows a result of a calculation of the net impurity density, after compensation of donor and acceptor centers. This figure illustrates the inversion from n-type to p-type with increased neutron fluence, and the eventual build-up of acceptors beyond the useful limit (solid curve). Also shown in Figure 13 by the dashed line is the affect of E-center formation within the material. Further, Figure 14 shows the expected neutron effects when self-annealing is taken into account. One has to assume the room temperature annealing time constants shown, but it poses a promising prospect for properly engineered devices. This work remains to be tested experimentally.

Conclusion

This short report has only scratched the surface of all the work done during the past year on SSC subsystem supported calorimetry with barium fluoride, scintillating fibers, liquid argon, liquid xenon/krypton, and silicon. We all trust that these efforts will be rewarded someday with spectacular new discoveries at the SSC.

Acknowledgments

The author acknowledges assistance from each of the subsystem projects in making results available. In particular, we thank Bill Bugg, Min Chen, Howard Gordon, Harvey Newman, Hans Paar, Adam Para, and Larry Sulak. This work was supported in part by the U.S. Department of Energy and the Texas National Research Laboratory Commission.

References

1. R.V. Steiner et al., "An Expression of Interest to Construct a Major SSC Detector," July 8, 1991, SSC EOI-0020.
2. J.E. Brau, K.T. Pitts, and L.E. Price, "Detection of Higgs Bosons decaying to Bottom Quarks at the SSC," Proceedings of the Summer Study on High Energy Physics in the 1990's, page 103, edited by Sharon Jensen, World Scientific, 1989.
3. C. Barter et al., "Detection of the $H^0 \rightarrow \gamma\gamma$ at the SSC," page 98, Proceedings of the Summer Study on High Energy Physics in the 1990's, page 103, edited by Sharon Jensen, World Scientific, 1989.
4. C.W. Fabjan, Lectures given at the NATO Advanced Studies Institute on Techniques and Concepts in High Energy Physics, St. Croix, Virgin Islands, USA, CERN-EP/85-54 (1985); C.W. Fabjan and R. Wigmans, Rept. Prog. Phys. 52, 1519 (1989).
5. D. Froidevaux, Proceedings of the Workshop on Physics at Future Accelerators, La Thuile and CERN, 1987, CERN 87-07, p 57.
6. R.M. Barnett et al., Proceedings of the Summer Study on High Energy Physics in the 1990s, Snowmass, Co., p. 159 (1989), ed. Sharon Jensen.
7. V. Barnes et al., Proceedings of the Workshop on Experiments, Detectors, and Experimental Areas for the Supercollider, Berkeley, California, p. 235 (1988).
8. H. Gordon et al., private communication.
9. G. Gratta et al., "A Precision BaF_2 Crystal Calorimeter for the Superconducting Supercollider," submitted to the SSC Laboratory, September, 1 1991.
10. Craig L. Woody, "A Report on Radiation Damage in Barium Fluoride to the GEM Collaboration," December 4, 1991.
11. R. Carey et al., "The Engineering and Testing of a Fiber Calorimeter Prototype For the Second Detector," submitted to the SSC Laboratory, September, 1991.
12. page 9, reference 11.
13. W. Worstell et al., "Cast Lead-eutectic Solid and Liquid Scintillating Fiber Shower Calorimeters," Proceedings of the Symposium on Detector Research and Development for the Superconducting Super Collider, Fort Worth,TX, October, 1990, page 428, edited by T. Dombeck, V. Kelly, and G.P. Yost (1991).
14. D. Acosta et al., "Effects of Radiation Damage on Scintillating Fiber Calorimetry," CERN-PPE/91-45 (1991).
15. R. Steiner et al., "Liquid Argon Calorimetry for the SSC," submitted to the SSC Laboratory, September, 1991.
16. V. Radeka and S. Rescia, Nucl. Inst. and Methods A265, 228 (1988).
17. H. Gordon et al., CERN 077C, August, 1988.
18. N.J. Hadley, "Test Beam Results for Liquid Argon Calorimetry with Fast Shaping," 1991 APS DPF Meeting, Vancouver, Canada (Appendix 1 of reference 15.)
19. K. Furuno, private communication and unpublished internal note.
20. P. Mockett, private communication and unpublished internal note.

21. SDC Liquid Argon Group, "SDC Calorimeter Conceptual Design, Liquid Argon Option," 5 August, 1991.
22. M. Chen et al., "Progress Report on Scintillating LXe/LKr EM Calorimeter," submitted to the SSC Laboratory, September, 1991.
23. B. Aubert et al., "Performance of a Liquid Argon Electromagnetic Calorimeter with an 'Accordion' Geometry," Nucl. Inst. and Methods A309, 438 (1991).
24. M. Chen, private communication.
25. H.W. Kraner et al., "Progress Report of the Silicon Electromagnetic Calorimeter Collaboration," submitted to the SSC Laboratory, September, 1991.
26. R.A. Todd et al., page 80, reference 25.
27. R. Wunstorf et al., "Results on Radiation Hardness of Silicon Detectors up to Neutron Fluences of 10^{15} n/cm^2," page 30 of [25].
28. H.W. Kraner and Zheng Li, page 48 of [25].
29. J. Walter, "Radiation Hardness," page 7 of [25].

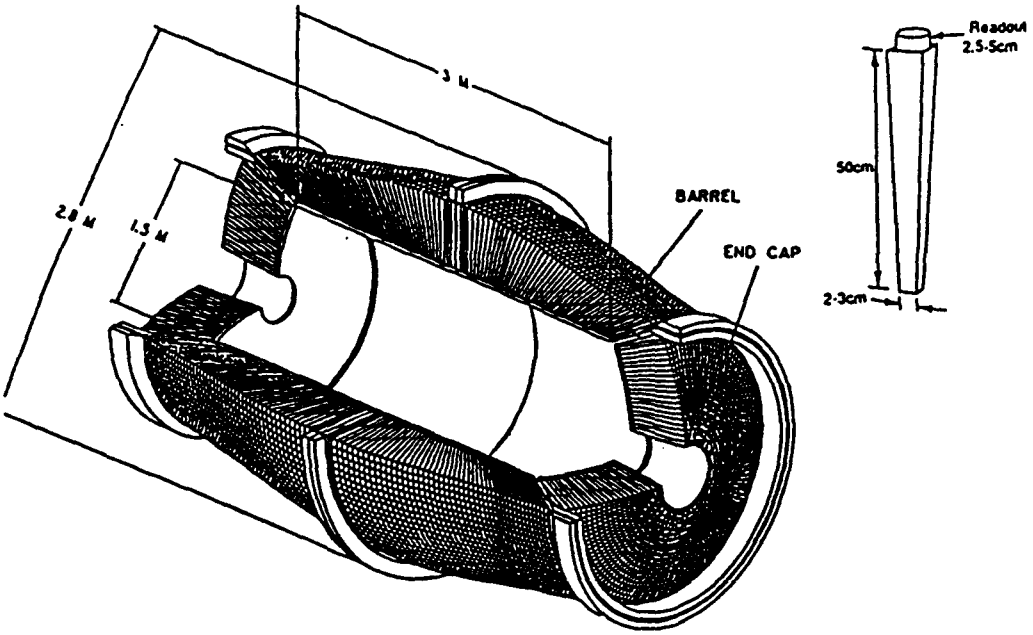

Figure 1. Conceptual view of the BaF_2 EM calorimeter

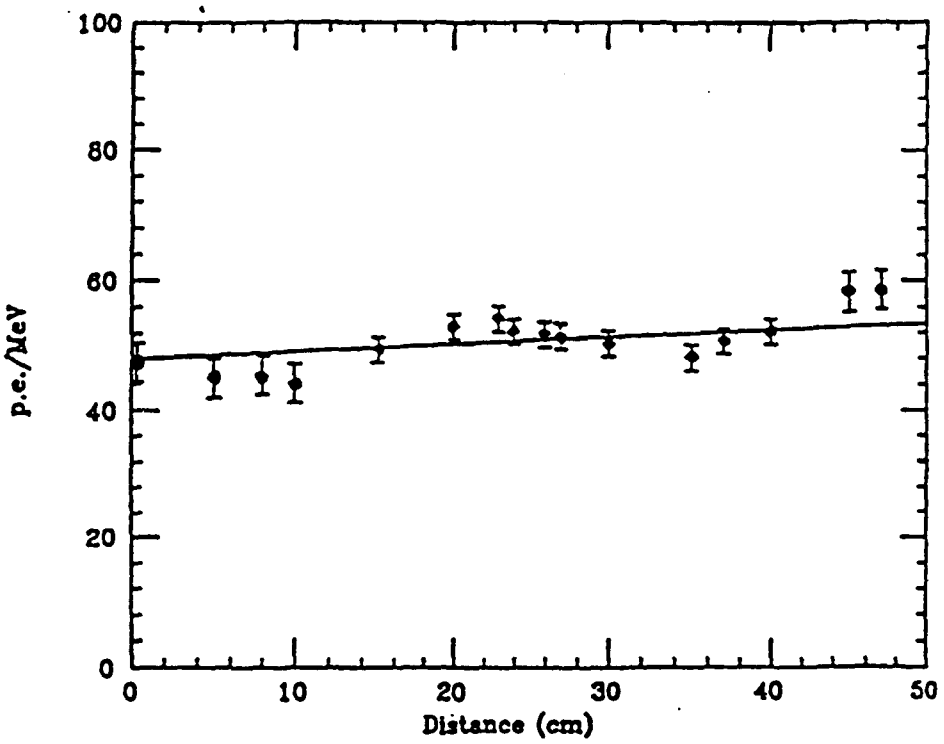

Figure 2. Photoelectrons/MeV obtained with a 50 cm crystal pair measured with a Cs^{137} source. x = 50 is near the phototube.

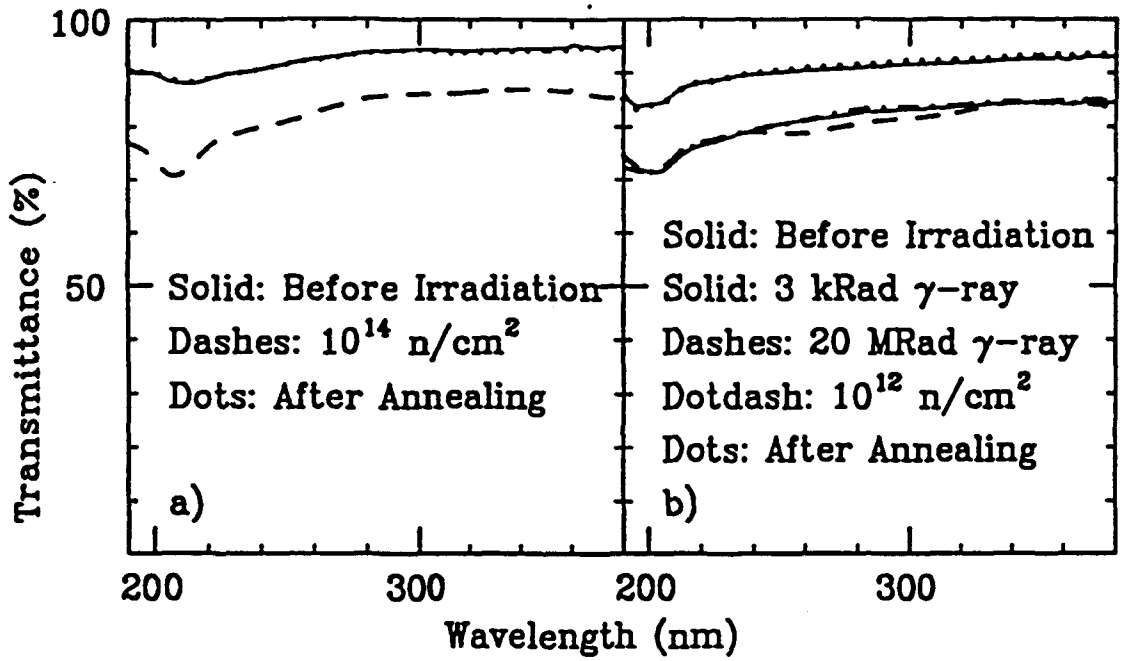

Figure 3. Transmittances before and after irradiation showing a) recovery from neutron damage and b) recovery from typical saturation effect.

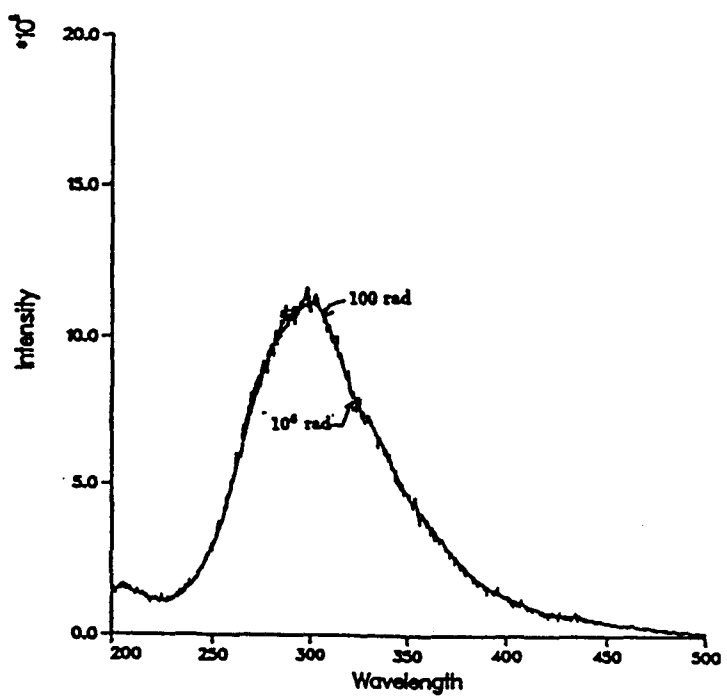

Figure 4. Scintillation emission spectrum for a 1" diameter by 1" long BaF_2 crystal measured during irradiation at 100 rad and 10^6 rad.

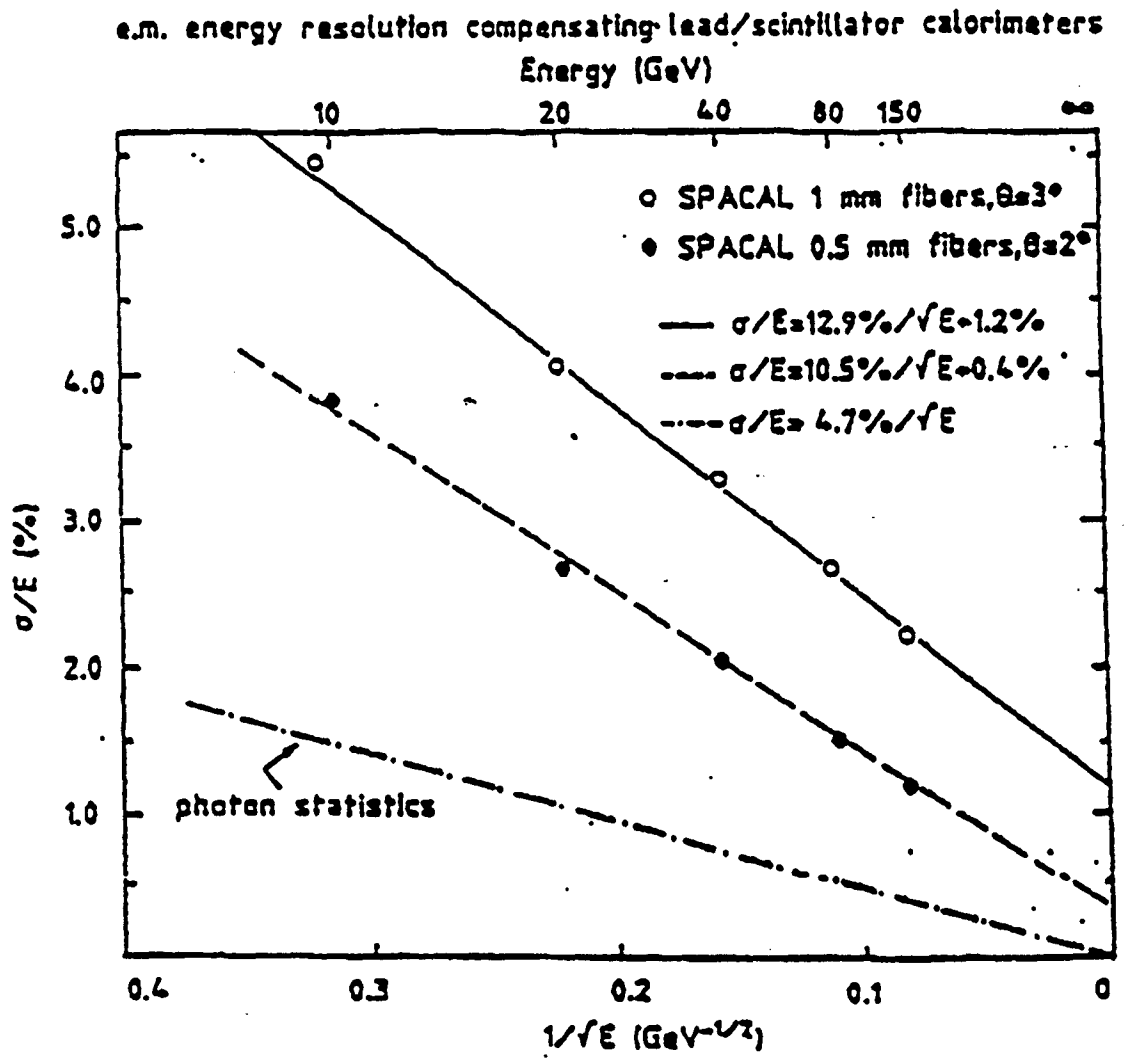

Figure 5. Preliminary energy resolution of a half millimeter scintillating fiber calorimeter prototype (solid dots) compared to the previous results with 1 millimeter fibers (open circles).[12]

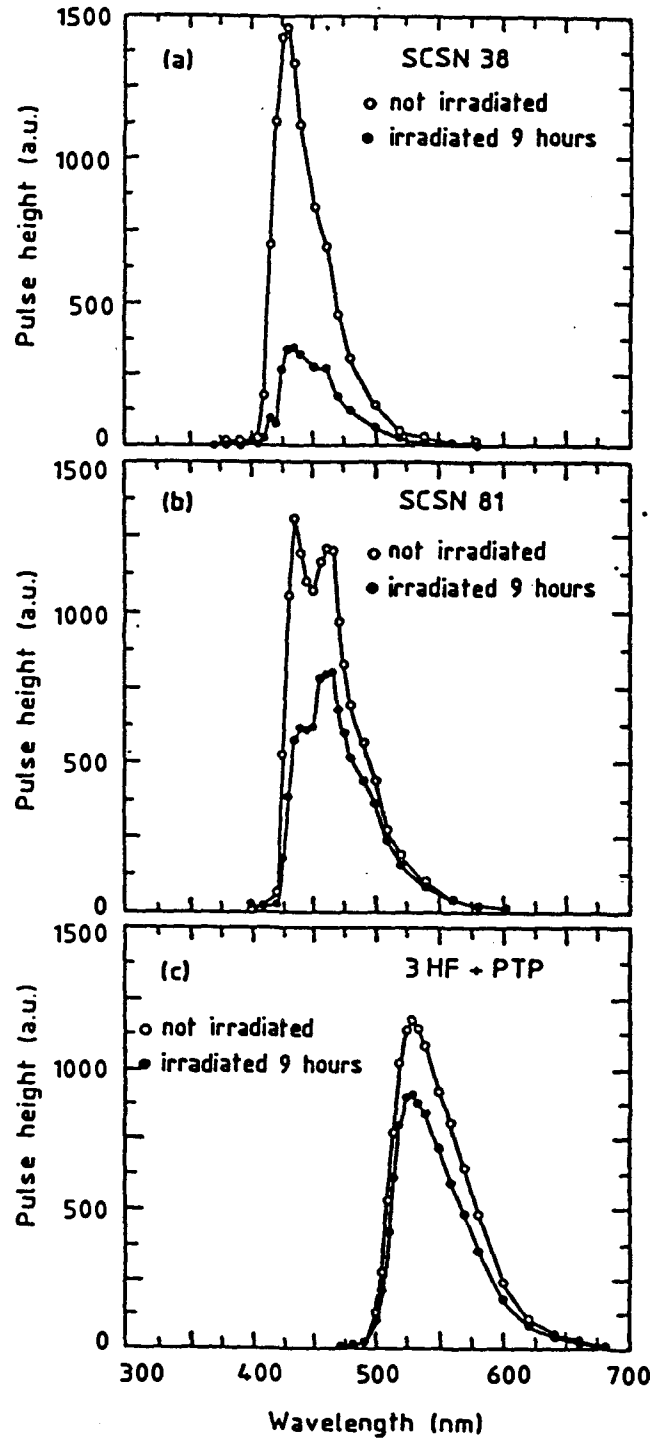

Figure 6. Wavelength spectra of scintillating fibers measured at 10 cm from the photomultiplier for a) SCSN38, b) SCSN81, and c) 3HF+PTP fibers before and after irradiation with a narrow dose profile. The total dose was 9.5 Mrad. See reference 14 for further details of the setup.

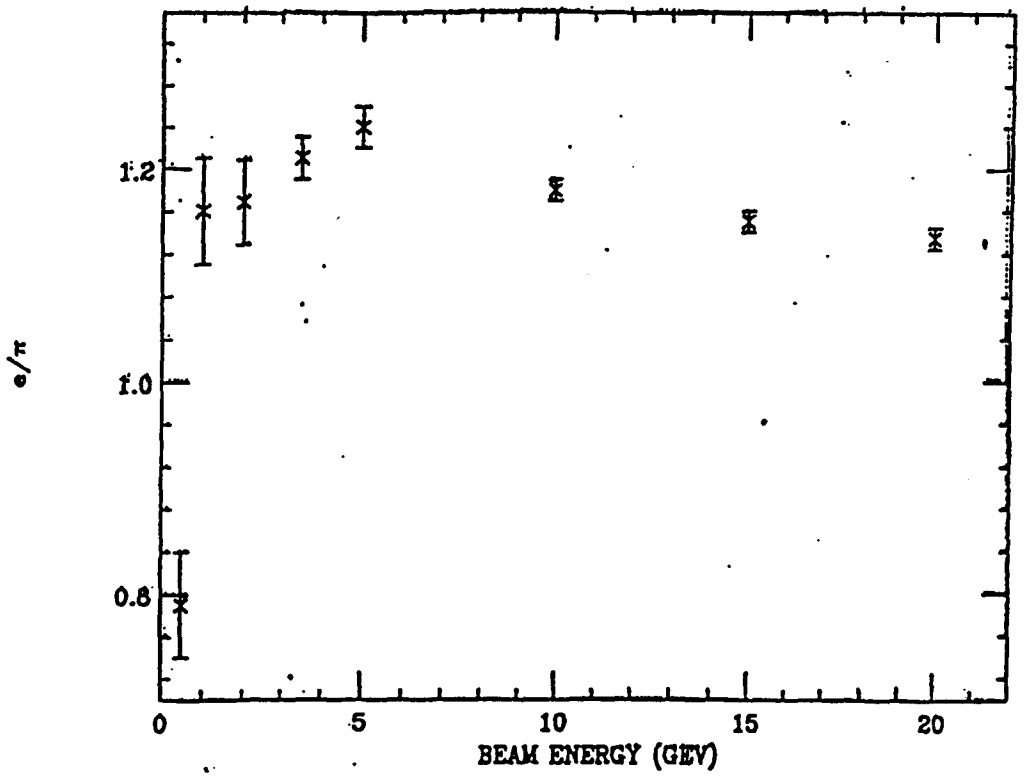

Figure 7. e/π as a function of momentum for the Liquid Argon Calorimeter tested at Brookhaven.

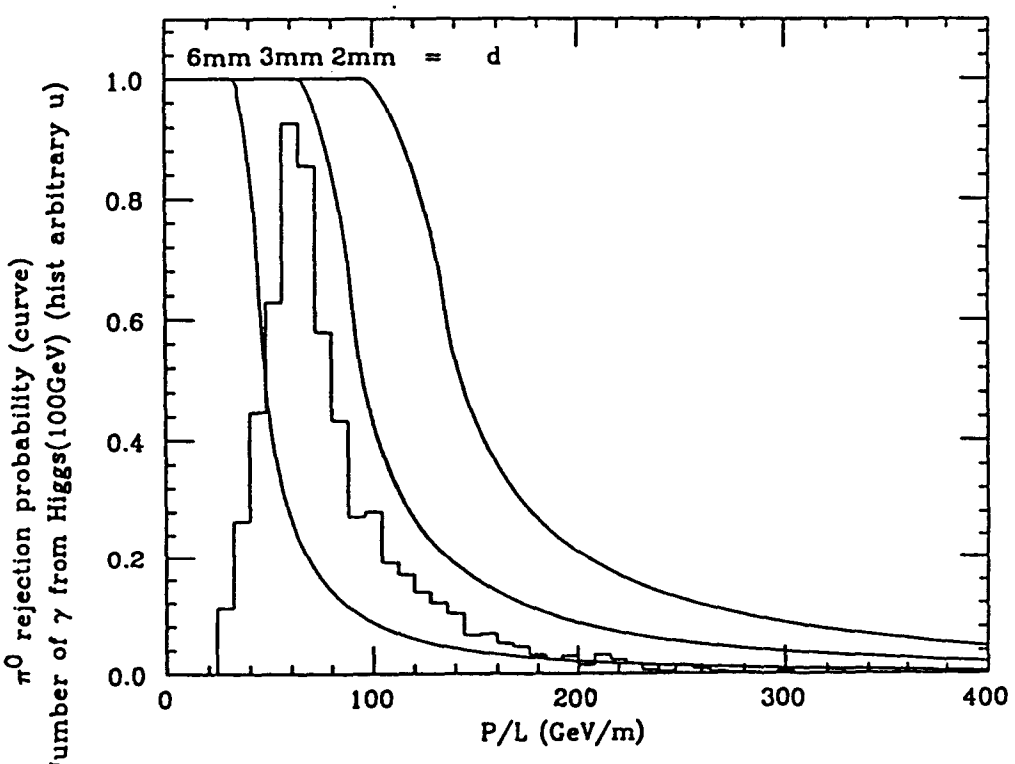

Figure 8. Preradiator π^0 rejection probability (curves) for GEM versus the momentum over path length. The histogram is the distribution of gammas from 100 GeV Higgs decays.

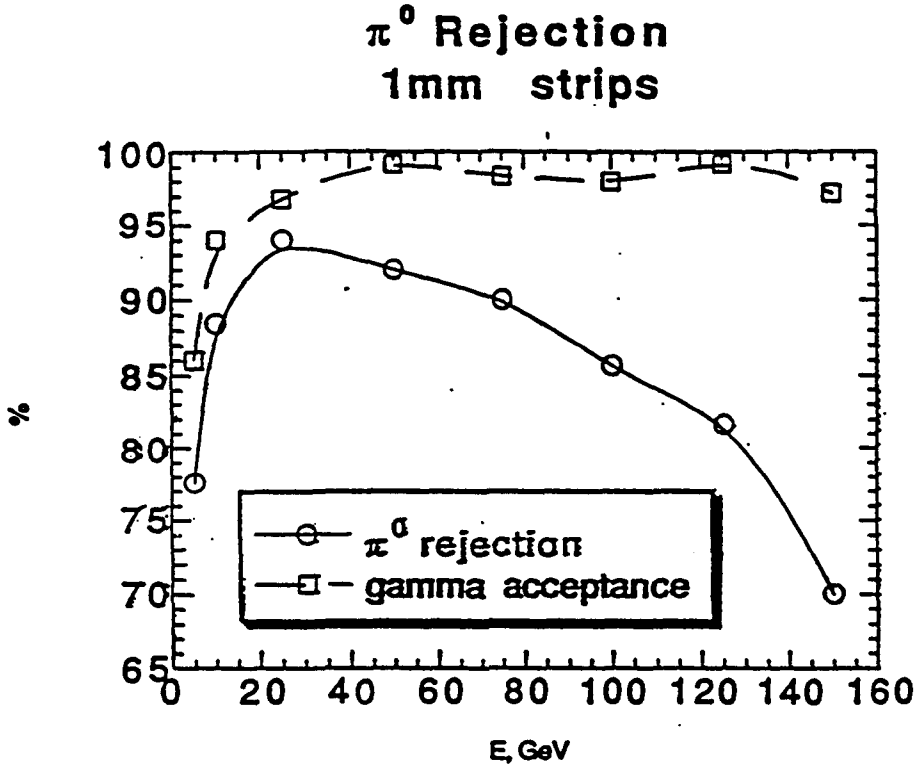

Figure 9. Liquid argon integrated preradiator π^0 rejection and gamma acceptance for 1 mm strips in the first 4 X_0 as a function of energy.

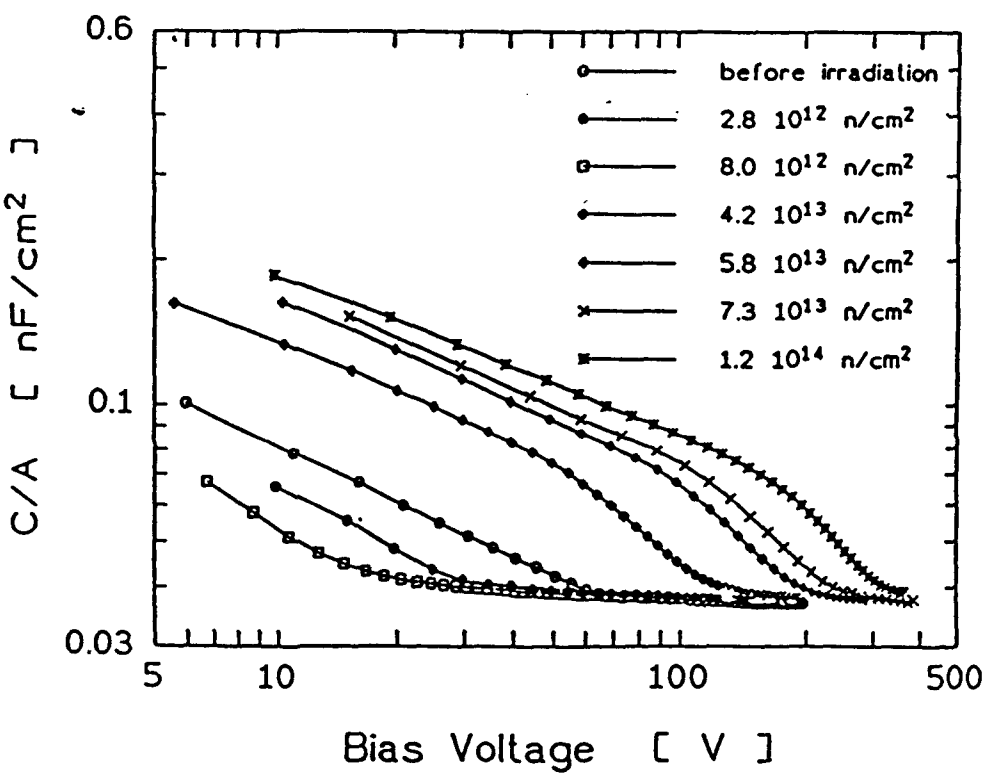

Figure 10. C/V characteristics measured at 10 kHz immediately after irradiation by various neutron fluences up to 1.2×10^{14} n/cm².[27]

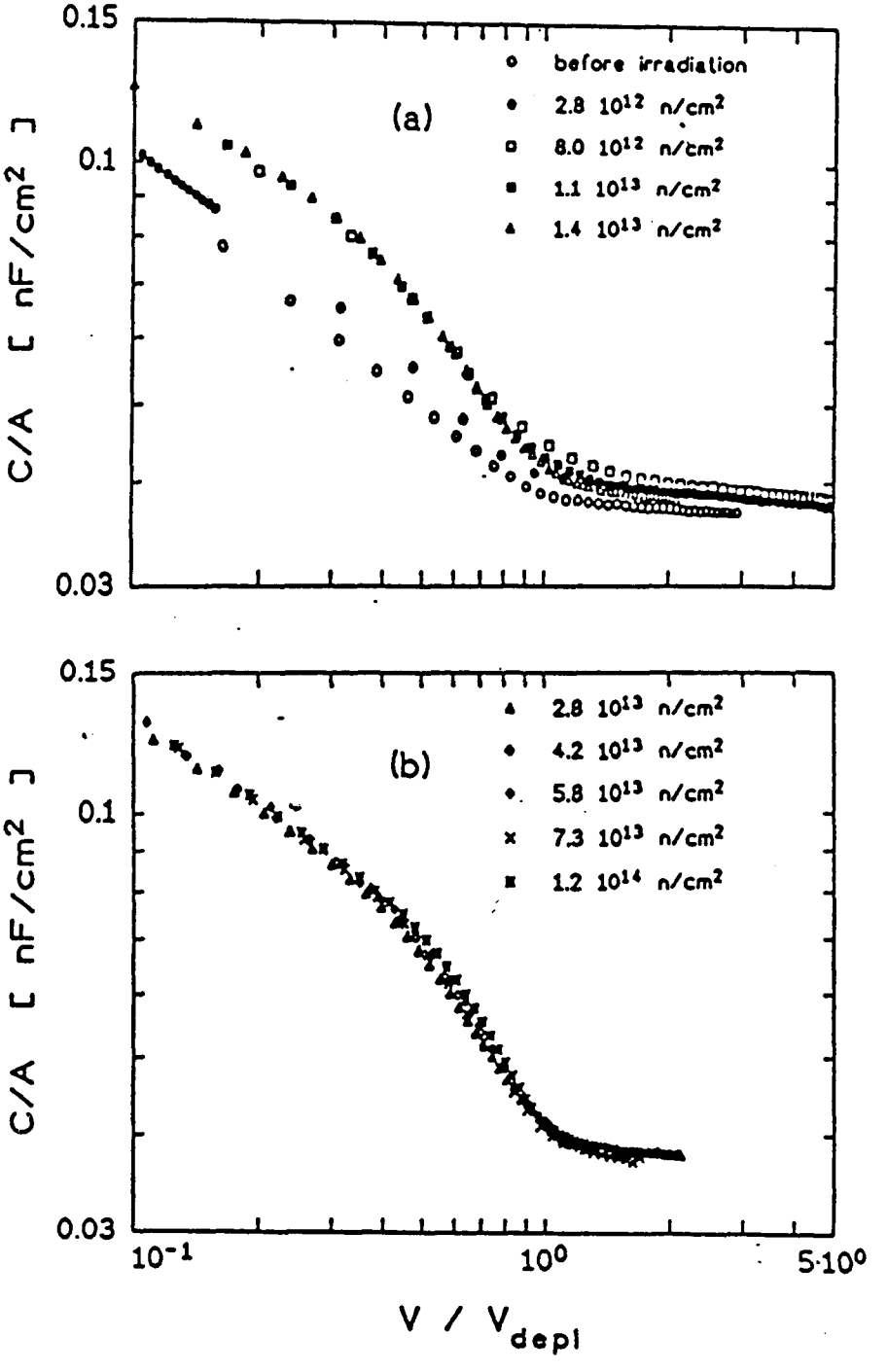

Figure 11. C/V characteristics shown in Figure 10 replotted as a function of the bias voltage normalized to the total depletion. [27]

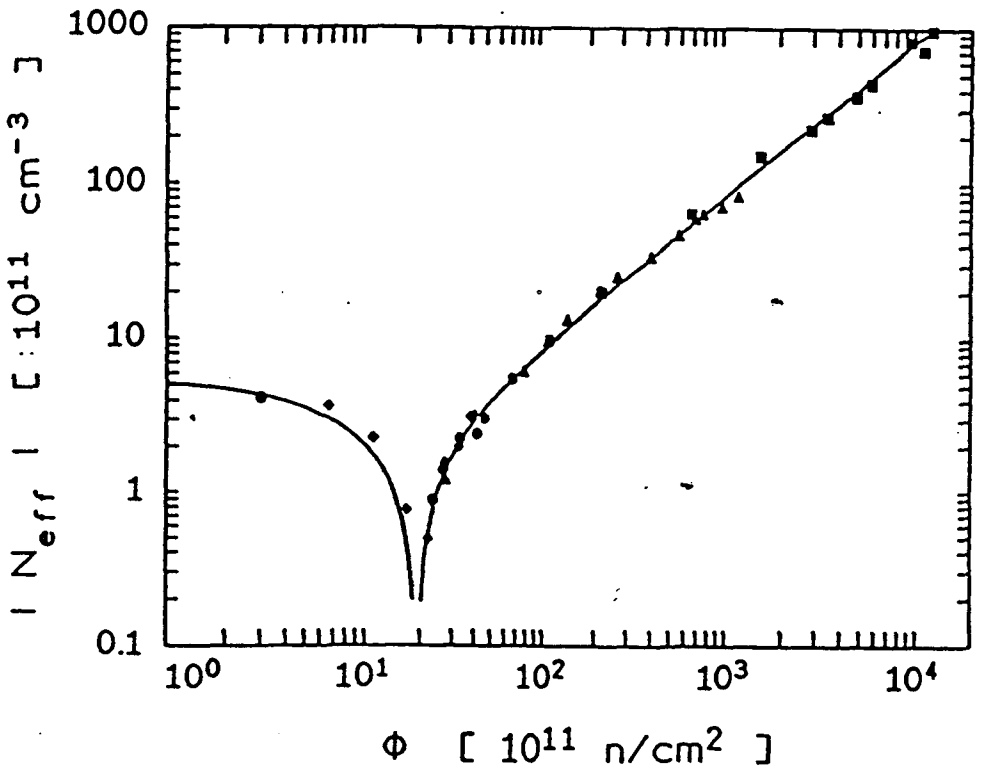

Figure 12. Absolute value of the effective impurity concentration versus fluence up to 10^{15} n/cm². The solid curve represents a fit to a model incorporating the removal of phosphorus donors and boron acceptors and a fluence proportional generation of acceptor like defects.[27]

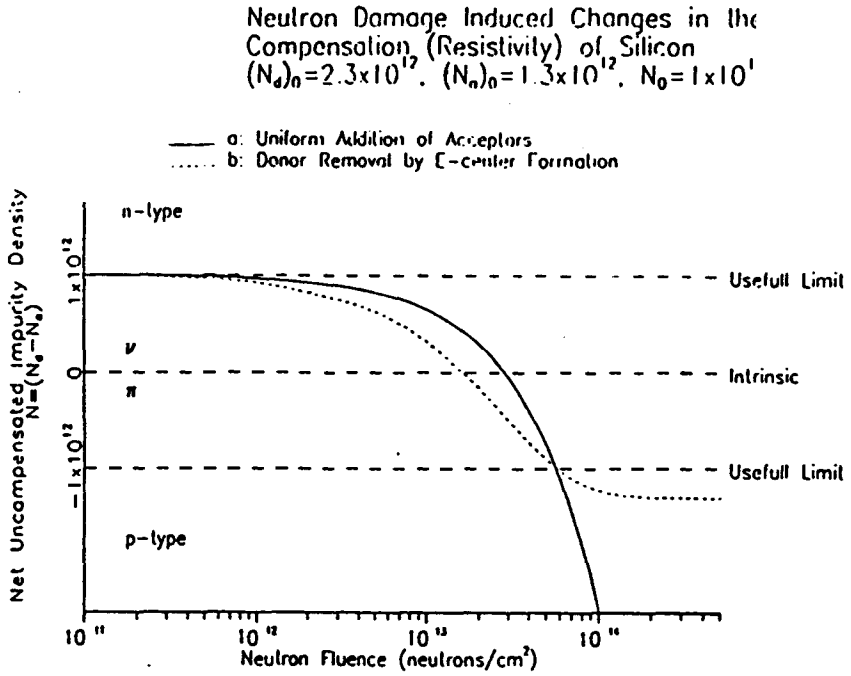

Figure 13. Neutron damage induced changes in the compensation (resistivity) of silicon for a model assuming uniform addition of acceptors (solid curve) and a model assuming donor removal by E-center formation.[29]

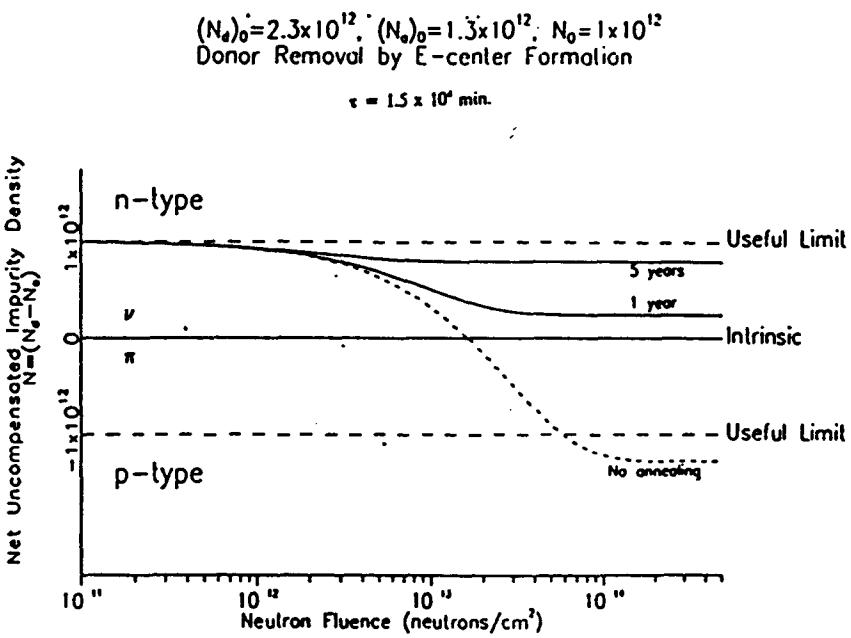

Figure 14. Neutron damage induced changes in the compensation (resistivity) of silicon for a model assuming donor removal by E-center formation, as in Figure 13. Here the effect of self-annealing is included.[29]